Journal of Alloys and Compounds 470 (2009) 63–66

Contents lists available at ScienceDirect

Journal of Alloys and Compounds

journal homepage: www.elsevier.com/locate/jallcom

Enhanced superconducting properties of bulk MgB_2 prepared by *in situ* Powder-In-Sealed-Tube method

Neson Varghese [a], K. Vinod [a], Ashok Rao [b], Y.K. Kuo [c], U. Syamaprasad [a,*]

[a] National Institute for Interdisciplinary Science and Technology (CSIR), Trivandrum 695019, India
[b] Department of Physics, Manipal Institute of Technology, Manipal 576104, India
[c] Department of Physics, National Dong Hwa University, Hualien 97401, Taiwan

ARTICLE INFO

Article history:
Received 11 January 2008
Received in revised form 6 March 2008
Accepted 7 March 2008
Available online 25 April 2008

PACS:
74.70.Ad
74.25.Ha
74.25.Sv

Keywords:
MgB_2 superconductor
Magnetic measurements
Critical current density

ABSTRACT

A systematic study on the superconducting properties of polycrystalline MgB_2 synthesized by *in situ* Powder-In-Sealed-Tube technique is carried out at different temperatures (750–900 °C). Both XRD and SEM results show well-crystallized MgB_2 grains in all the samples and grain size is found to be increasing with the sintering temperature. Sharp superconducting transitions are observed for all samples, irrespective of sintering temperatures, which implies the high degree phase purity and homogeneity of MgB_2 formed, while $J_C(H)$ plot gives sample dependent critical current density. The samples heat treated at relatively low temperatures show enhanced flux pinning and hence improved $J_C(H)$ performance. The reduced grain size and hence increased density of grain boundary pinning centers of MgB_2 bulks synthesized at low temperature are mainly responsible for the enhanced flux pinning and J_C.

1. Introduction

With a relatively high critical temperature (T_C) of 39 K [1], much higher than that of low temperature superconductors (LTS), MgB_2 is a promising candidate for large-scale applications at 20 K. As compared to oxide superconductors, MgB_2 has simple crystal structure and less anisotropy than layered HTS, thus minimizing effect of grain boundaries on superconducting properties. The usefulness of MgB_2 for practical applications is based mainly on its lightness, low cost, suitable mechanical and metal-like properties and amenability for preparing wires and tapes.

Considerable efforts are put on the synthesis of samples in the form of bulk, thin film, tape and wire [2]. The properties of bulk MgB_2 mainly depends on purity, size distribution and homogeneity of precursor powder, fabrication procedure and heat treatment schedule. There are two main routes to prepare bulk MgB_2, based on the reaction of pure elements (*in situ* technique) and the sintering of pre-reacted MgB_2 powders (*ex situ* technique). Of which *in situ* method is more preferred since it provides better grain connectivity and effective control of pinning centers. Improvement in critical current density ($J_C(H)$), upper critical field (H_{C2}) and irreversibility field (H_{irr}) is the key factor for practical applications of MgB_2 superconductor and this depends sensitively on flux pinning, grain connectivity, density, chemical composition and microstructure. MgO phase at the grain boundaries is the major impurity in the *in situ* synthesized MgB_2 that severely affects the J_C. The MgO at the grain boundaries acts as weak links and significantly reduce the intergrain J_C [3].

Several synthesis procedures have been reported for *in situ* bulk MgB_2 synthesis. Generally, the synthesis is done by enclosing samples in Nb/Ta tubes or foils in inert atmosphere or vacuum. The maximum J_C reported is only in the range 10^3–10^4 A/cm^2 at 20 K and 2 T [4–7]. This is due to high volatility of Mg at elevated temperatures resulting in high porosity and poor superconducting properties. Although reasonably dense bulk MgB_2 samples were obtained under hot pressing of specimen at high pressure and high temperature ($J_C \sim 10^5$–10^6 A/cm^2 at 20 K and 2 T) [8–11], the large-scale exploitation of MgB_2 as a potential material for various practical applications requires development of more simple and cost-effective processing techniques. The method we used for bulk MgB_2 synthesis is *in situ* Powder-In-Sealed-Tube (PIST) technique in which the ends of the powder-filled tubes were pressed and sealed by 'cold-welding' so that the samples can be heat treated directly in air [12]. This can practically eliminate Mg evaporation

* Corresponding author. Tel.: +91 471 2515373; fax: +91 471 2491712.
E-mail address: syamcsir@gmail.com (U. Syamaprasad).

0925-8388/$ – see front matter © 2008 Elsevier B.V. All rights reserved.
doi:10.1016/j.jallcom.2008.03.056

loss and minimize oxidation of Mg and reduce the cost of synthesis by avoiding expensive Nb/Ta tubes or foils, inert gases and special furnaces. For *in situ* synthesis of MgB_2, the synthesis conditions have strong influence on the phase formation, crystallinity and microstructure and hence on the superconducting properties of the material. In this work, we study the superconducting properties of bulk MgB_2 synthesized at different temperatures by *in situ* Powder-In-Sealed-Tube technique.

2. Experimental details

Bulk MgB_2 samples were prepared by *in situ* Powder-In-Sealed-Tube (PIST) method. Commercially available SUS 304 tubes of 10 cm long with an outside diameter (OD) of 10 mm and inside diameter (ID) of 8 mm were used for synthesis. One end of tube was pressed uniaxially using a hydraulic press so that it became tape shaped. Stoichiometric weights of commercially available Mg powder (−325 mesh, 99.8%) and boron powder (−325 mesh, 99%, amorphous) were taken using an electronic balance (Mettler AE240). Powders were mixed and ground thoroughly in air for about 30 min to get homogeneous fine powder using an agate mortar and pestle. Then the powder mixture was densely packed through the open end of the pressed stainless steel tube leaving some space unfilled. The unfilled portion was pressed with the same pressure as that of previous end such that both the pressed ends are of equal length. Subsequently, the powder-filled middle area was again subjected to uniaxial pressing to get a tape shaped portion. End sealing was performed by arc welding in order to avoid the escape of volatile Mg. A wet cloth was wound around the specimen during welding to avoid heating up of the sample. Samples were then heat treated directly in air at 750, 800, 850, and 900 °C for 2 h in a muffle furnace with a ramp rate of 10 °C/min and subsequently performed furnace cooling. Bar shaped MgB_2 core was taken out by mechanically peeling off the SS sheath for X-ray, SEM and magnetic measurements. The samples heat treated at 750, 800, 850, and 900 °C for 2 h are named as MB750, MB800, MB850, and MB900, respectively.

The structural and phase analysis of the samples were performed using an X-ray diffractometer (Philips X'pert Pro) with Cu Kα radiation employing X'Celerator and monochromator at the diffracted beam side. Phase identification of the samples was performed using X'Pert Highscore Software in support with ICDD-PDF-2 database. The microstructure and homogeneity of the samples were examined using a scanning electron microscope (SEM-JEOL JSM 5600 LV). DC magnetic measurements were carried out using a SQUID based magnetometer on cut pieces of 4 mm × 3 mm × 1.5 mm, with applied field along the longest dimension.

3. Results and discussion

Fig. 1 shows powder XRD patterns of the samples heat treated at different temperatures 750, 800, 850, and 900 °C for 2 h. All X-ray diffraction pattern show sharp peaks of MgB_2 phase with only a minute fraction of MgO. Traces of MgO observed are due to the entrapped air in the reaction mixture before end-sealing of the tubes. Small amount of unreacted residual Mg is detected for the sample heat treated at 750 °C. However, MgB_2 peaks become sharper and stronger as the heat treatment temperature increases, which indicate increase in phase purity and/or crystallinity. No peaks of MgB_4 or other higher borides in all samples confirm that there is no evaporation of Mg during the heat treatment process. Table 1 shows the lattice parameters *a*, *c* axes and full width at half maximum (FWHM) of the (1 0 0), (1 0 1), (0 0 2) and (1 1 0) peaks of the samples. The lattice parameters are calculated from XRD for

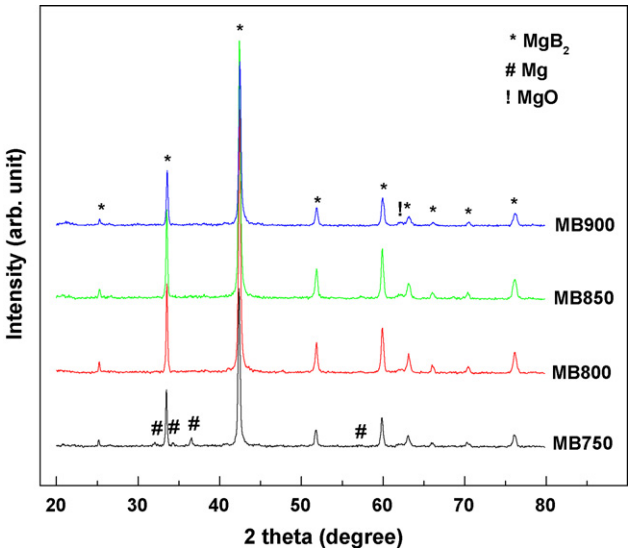

Fig. 1. XRD patterns of MgB_2 samples heat treated at different temperatures 750, 800, 850, and 900 °C for 2 h.

hexagonal structure with space group *p*6/*mmm*. FWHM of all the peaks decreases significantly with increasing the sintering temperature indicating the increase in grain size of MgB_2 with sintering temperature. Fig. 2 shows typical secondary electron SEM images of the samples heat treated at 800 and 900 °C. The microstructure of the samples is homogenous in nature. The samples show fine hexagonal and randomly oriented MgB_2 grains. SEM images also show that the average grain size of the crystalline MgB_2 increases with sintering temperature, well in agreement with decrease of FWHM from XRD.

Temperature dependence of magnetization (*M*–*T*) of the samples is shown in Fig. 3. All the samples show sharp superconducting transition with T_C around 38.5 K and ΔT_C ($T_{C90\%} - T_{C10\%}$) ~ 0.8 K indicating the high phase purity and homogeneity of MgB_2 samples sintered at different temperatures. Almost identical T_C and ΔT_C values of the samples indicate that the stoichiometry of all the samples are same and samples are identical with respect to lattice or structural defects and the electronic states in the superconducting B planes. The critical current density J_C of the bulk MgB_2 samples was calculated from the width of the magnetization hysterisis (*M*–*H*) loops on the basis of the Bean critical state model using the relation

$$J_C(H) = \frac{20\Delta M}{a(1 - a/3b)},$$

where $a < b$, ΔM is the width of *M*–*H* loop and *a* and *b* are dimensions of the parallelopiped sample perpendicular to the field [13].

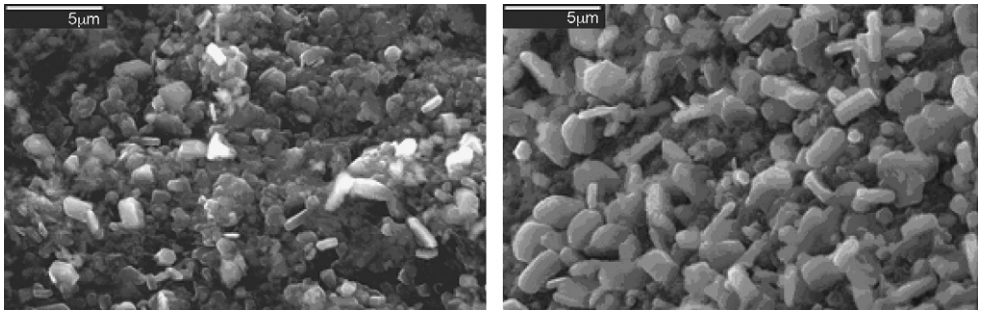

Fig. 2. Typical secondary electron SEM images of the samples heat treated at 800 and 900 °C.

Table 1
Lattice parameters *a* and *c* axes and full width at half maximum (FWHM) of the larger peaks of MgB_2 samples

Sample	*a* (Å)	*c* (Å)	FWHM (°)			
			(1 0 0) Peak	(1 0 1) Peak	(0 0 2) Peak	(1 1 0) Peak
MB750	3.0865	3.5236	0.2218	0.2820	0.3281	0.3273
MB800	3.0877	3.5212	0.2115	0.2642	0.3056	0.3172
MB850	3.0872	3.5233	0.2049	0.2507	0.2859	0.3083
MB900	3.0897	3.5185	0.1833	0.2279	0.2558	0.2367

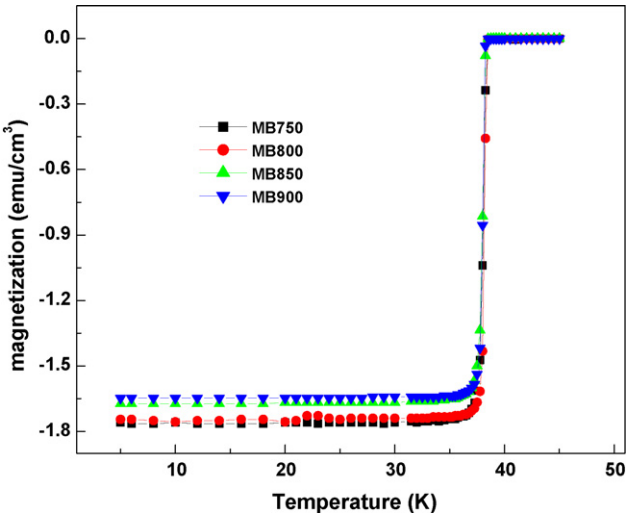

Fig. 3. DC magnetic susceptibility versus temperature plots in both zero field cooled (ZFC) conditions at 20 Oe for MgB_2 samples.

Fig. 4 illustrates the dependence of J_C with applied magnetic fields upto 5 T of MgB_2 samples at 10 and 20 K. At 10 K, J_C jumps abruptly at low fields where the estimation of J_C may not be accurate due to the flux jumps, whereas $J_C(H)$ follows a systematic behavior in higher fields for all samples. Sample heat treated at 800 °C shows the highest J_C in external fields at both 10 and 20 K. It is found that the $J_C(H)$ performance is better for samples heat treated at lower sintering temperatures (750 and 800 °C), while it is lower for samples heat treated at higher sintering temperatures (850 and 900 °C).

Fig. 5 shows the normalized flux pinning force density f_p ($F_P/F_{P_{max}}$, where $F_P = J_C \times B$) with applied magnetic field (H) of the

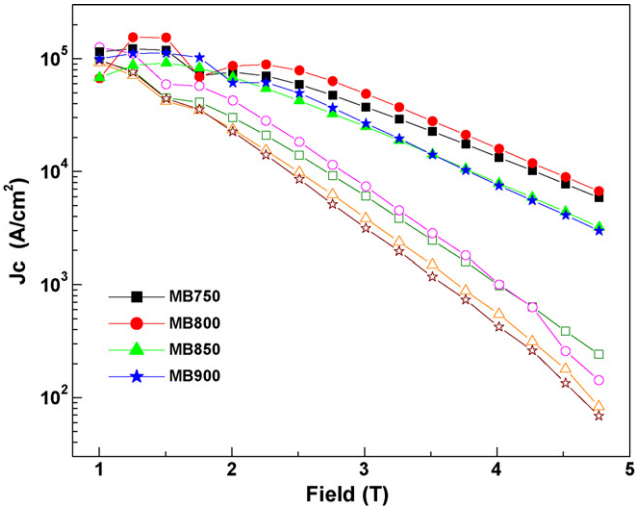

Fig. 4. $J_C(H)$ curves of MgB_2 samples synthesized at different temperatures. Closed and open symbols represent $J_C(H)$ at 10 and 20 K, respectively.

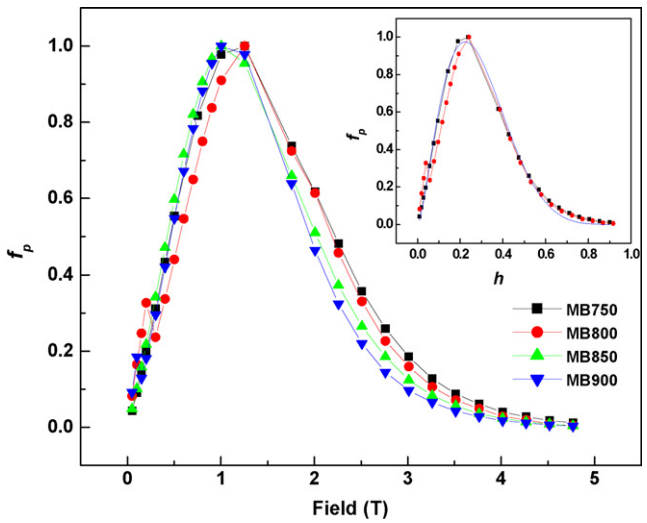

Fig. 5. Normalized flux pinning force density fp versus magnetic field at 20 K for MgB2 samples. Inset shows normalized flux pinning force density f_p versus reduced field h for MB750 and MB800 at 20 K and for the theoretical fitting (straight line) of the formula $f_p \propto h^p(1-h)^q$.

samples. The flux pinning curves show a linear nature at lower fields upto a maximum pinning force density after which the curves exhibit a quadratic behavior at higher fields, typical for MgB_2 samples. The figure clearly shows enhanced pinning at higher fields for the samples heat treated at lower sintering temperatures (MB750 and MB800) as compared to that of the samples heat treated at higher sintering temperatures (MB850 and MB900). Normalized flux pinning force density f_p ($F_P/F_{P_{max}}$) verses reduced field h (H/H_{irr}) for MB800 at 20 K and for the theoretical fitting of the formula $f_p \propto h^p(1-h)^q$ is shown in inset of Fig. 5. The value of H_{irr} is obtained by linear extrapolation of Kramer curves, $J_C^{1/2}H^{1/4}(H)$ [14]. The peak of the f_p curve takes place at $h \sim 0.2$ which seems that normal surface pinning (grain boundary) is the dominant pinning mechanism in bulk MgB_2. The f_p curve of MB800 sample is fitted well with the function $f_p \propto h^p(1-h)^q$, where $p = 1.3$ and $q = 4.5$. This behavior has been also observed by other groups in MgB_2 [15–17]. From the FWHM and SEM images, it is clear that the average grain sizes of MB750 and MB800 are comparably smaller than that of MB850 and MB900. Thus, the reduced grain size and hence increased grain boundaries of MB750 and MB800 is the reason for the improved pinning and $J_C(H)$ in these samples.

Fig. 6 compares J_C with applied magnetic field at 20 K for bulk *in situ* MgB_2 samples (PIST) in this work and from literature with respect to various synthesize routes [4–11]. Our sample shows higher $J_C(H)$ performance as compared to other preparation methods including low pressure and high pressure synthesis except for hot isostatic pressed (HIP) sample [11]. In bulk MgB_2 HIPed sample, large bulk density and less amount of voids are the main reasons for obtaining high J_C. Dou and co-workers reported comparable or slightly higher J_C for MgB_2 bulk samples and studies by them showed that the presence of more MgO content reduces T_C and

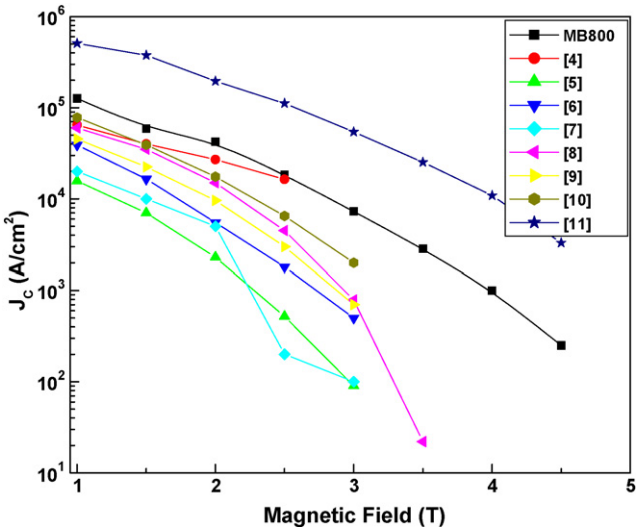

Fig. 6. Comparison of J_C versus applied magnetic field at 20 K for bulk *in situ* MgB_2 samples in this work and from literature [4–11].

improves J_C [4]. $J_C(H)$ performance of other preparative methods such as pellets/Ta tube at 1200 °C/8 h in vacuum [5], powder/SS tube at 825 °C/6 h [6], pellets liquid-assisted sintered at 950 °C/15 min [7], high pressure synthesis (2 GPa) at 950 °C/1 h [8], high pressure synthesis (4.5 GPa) at 850 °C/1 h [9] and hot deformation from 850 to 900 °C [10] are well below of our PIST method. The estimation of J_C below 1 T is difficult due to flux jump and more stabilization of flux jump is needed to obtain precise J_C at lower fields. The high phase purity and homogeneity of the MgB_2 samples yielded by *in situ* PIST method propose further flux pinning studies which may stabilize flux jump and enhance J_C for bulk MgB_2. This method is suitable for systematic studies of the various effects on MgB_2 by magnetic and transport measurements. Overall, the results show that the PIST method offers high quality bulk MgB_2 with the better $J_C(H)$ behavior in addition to reduction of complexity and cost of the whole manufacturing procedure.

4. Conclusion

The superconducting properties of bulk *in situ* PIST MgB_2 at different temperatures are studied. XRD analysis gives sharp peaks of MgB_2 phase with only a minute fraction of MgO. Well-crystallized MgB_2 grains are formed in all the samples prepared at temperatures in the range 750–900 °C and the grain size is found to increase with the temperature. All samples show sharp diamagnetic transition at 38.5 K, independent of samples where the in field critical current density shows a distinct dependence on the samples heat treated at different temperatures. The samples heat treated at relatively lower temperatures showed enhanced flux pinning and hence improved $J_C(H)$ performance. The reduced grain size and hence increased grain boundary is main reason for the improved flux pinning and $J_C(H)$ for the samples sintered at lower temperatures.

Acknowledgment

The authors Neson Varghese and K. Vinod acknowledge Council of Scientific and Industrial Research (CSIR), India for providing research fellowships.

References

[1] J. Nagamatsu, N. Nakagawa, T. Muranaka, Y. Zenitani, J. Akimitsu, Nature 410 (2001) 63.
[2] K. Vinod, R.G. Abhilash Kumar, U. Syamaprasad, Supercond. Sci. Technol. 20 (2007) R1.
[3] S. Hata, T. Yoshidome, H. Sosiati, Y. Tomokiyo, N. Kuwano, A. Matsumoto, H. Kitaguchi, H. Kumakura, Supercond. Sci. Technol. 19 (2006) 161.
[4] R. Zeng, L. Lu, J.L. Wang, J. Horvat, W.X. Li, D.Q. Shi, S.X. Dou, M. Tomsic, M. Rindfleisch, Supercond. Sci. Technol. 20 (2007) L43.
[5] P.C. Canfield, S.L. Budko, D.K. Finnemore, Physica C 385 (2003) 1.
[6] S. Ueda, J. Shimoyama, A. Yamamoto, S. Horii, K. Kishio, Supercond. Sci. Technol. 17 (2004) 926.
[7] S.K. Chen, Z. Lockman, M. Wei, B.A. Glowacki, J.L.M. Driscoll, Appl. Phys. Lett. 86 (2005) 242501.
[8] T.A. Prikhna, W. Gawalek, Y.M. Savchuk, V.E. Moshchil, N.V. Sergienko, A.B. Surzhenko, M. Wendt, S.N. Dub, V.S. Melnikov, C. Schmidt, P.A. Nagorny, Physica C 386 (2003) 565.
[9] M. Dhalle, P. Toulemonde, C. Beneduce, N. Musolino, M. Decroux, R. Flukiger, Physica C 363 (2001) 155.
[10] A. Handstein, D. Hinz, G. Fuchs, K.H. Muller, K. Nenkov, O. Gutfleisch, V.N. Narozhnyi, L. Schultz, J. Alloys Compd. 329 (2001) 285.
[11] X.L. Wang, S. Soltanian, M. James, M.J. Qin, J. Horvat, Q.W. Yao, H.K. Liu, S.X. Dou, Physica C 408–410 (2004) 63.
[12] R.G. Abhilashkumar, K. Vinod, R.P. Aloysius, U. Syamaprasad, Mater. Lett. 60 (2006) 3328.
[13] C.P. Bean, Phys. Rev. Lett. 8 (1962) 250.
[14] D.C. Larbalestier, et al., Nature 410 (2001) 186.
[15] S. Keshavarzi, M.J. Qin, S. Soltanian, H.K. Liu, S.X. Dou, Physica C 408–410 (2004) 601.
[16] D.A. Cardwell, N. Hari Babu, M. Kambara, A.M. Campbell, Physica C 372–376 (2002) 1262.
[17] W.X. Li, R.H. Chen, Y. Li, M.Y. Zhu, H.M. Jin, R. Zeng, S.X. Dou, B. Lu, J. Appl. Phys. 103 (2008) 013511.